Available online at www.sciencedirect.com

ScienceDirect

Materials Today: Proceedings 6 (2019) 242–249

materialstoday: PROCEEDINGS

www.materialstoday.com/proceedings

3rd ISE SSRSEU 2018

The comparative study of electrocatalytic activity of various anode materials in respect to the oxidation of nitroanilines

S. Zahorulko[a], O. Shmychkova[a], T. Luk'yanenko[a], L. Dmitrikova[b], A. Velichenko[a,*]

[a] *Ukrainian State University of Chemical Technology, 8, Gagarin Ave., 49005 Dnipro, Ukraine*
[b] *Oles Honchar Dnipro National University, 72, Gagarin Ave., 49010 Dnipro, Ukraine*

Abstract

The comparative study of electrocatalytic activity of DSA, lead dioxide and F-PbO_2 has been performed. It has been shown that the processes of electrochemical oxidation of nitroanilines on investigated materials occur qualitatively the same and differ only in the rate. This suggests the invariability of the mechanism of their oxidation on different materials that allows one for a correct comparison of their electrocatalytic activity. The maximum interest for the electrochemical destruction of nitroanilines represents lead dioxide electrodes modified by fluorine to which a rate constant of p-nitroaniline oxidation increases in 3 times compared with nonmodified electrodes.

Selection and peer-review under responsibility of the scientific committee of 3rd ISE Satellite Student Regional Symposium on Electrochemistry in Ukraine.

Keywords: Lead dioxide; DSA; methanesulfonate electrolyte; oxygen evolution; electrooxidation of organic compounds

1. Introduction

Nitroanilines are widely used in industrial organic synthesis as reagents or intermediates [1]. For example, as diazo-components in the synthesis of azo dyes, as intermediates in the production of dispersed and cationic dyes, pigments, optical brighteners; as corrosion inhibitors; in the production of a number of antioxidants, additives to fuel, pesticides, antiseptics, agrochemicals, pharmaceuticals [1-4].

* Corresponding author. Tel.: +380562473627.
E-mail address: velichenko@ukr.net

Selection and peer-review under responsibility of the scientific committee of 3rd ISE Satellite Student Regional Symposium on Electrochemistry in Ukraine.

Since nitroanilines are highly toxic, and have carcinogenic and mutagenic effects, the issue of wastewater treatment from them is topical. However, chemical, physical and biological purification methods are resulted in incomplete destruction of nitroanilines, which leads to the formation of secondary contaminants [5, 6].

Secondary oxidation methods allow the mineralization of aromatic compounds to CO_2, H_2O and inorganic components or convert them to simple mono- and dicarboxylic acids, which can be mineralized by further biological purification. Therefore, these methods are recognized to be very promising in wastewater treatment. Often, an electrochemically generated Fenton reagent is used for the destruction of aromatic compounds [7]. It was shown in series of works [7-9], that electro-photo-Fenton is most effective in acid media (pH = 2−3).

As it has been shown in [10], the photodestruction of p-nitroaniline proceeds with a rate constant of 2.59×10^{-2} min^{-1}. The hydrothermal decomposition of p-nitroaniline (PNA) is a first-order reaction and occurs mainly with the formation of CO, CO_2, NH_3, and trace amounts of NO^{3-}, NO^{2-}, N_2, 5-methyl-2-pyridylamine and aniline [11]. Oxidation of p-nitroaniline using Fenton's reagent is also a pseudo-first order reaction [10]. Applying the quasi-stationary approximation to the process of oxidation of p-nitroaniline, the reaction order can be simplified to zero with respect to the PNA if the concentration of the latter is sufficiently large. At the ratio $[H_2O_2]/[PNA]$ = 55:1, oxidation can be considered as a pseudo-first order reaction [10]. Oxidation of nitroanilines proceeds more efficiently when the substituents are in direct polar conjugation [9].

Herein, we report further important details on the effect of anode material on the electrocatalytic activity in reactions proceeding at high anodic potentials with oxygen-containing particles participation, namely the electrooxidation of o-nitroaniline and p-nitroaniline (ONA and PNA, respectively).

2. Material and methods

All chemicals were reagent grade. Lead dioxide anodes were synthesized according to the method described elsewhere [12−14] by electrochemical deposition of PbO_2 on a platinized titanium substrate. Lead dioxide was electrodeposited methanesulfonate / nitrate electrolytes that contained 0.1 M CH_3SO_3H / HNO_3, 0.1 M $Pb(CH_3SO_3)_2$ / $Pb(NO_3)_2$. NaF was used as an additive to the electrolyte.

X-ray powder diffraction data were collected on a STOE STADI P automatic diffractometer equipped with linear PSD detector (transmission mode, 2θ/ω-scan; Cu $K\alpha_1$ radiation, curved germanium (1 1 1) monochromator; 2θ-range 6.000≤2θ≤102.945 °2θ with step 0.015 °2θ; PSD step 0.480 °2θ, scan time 50 s/step).

Qualitative and quantitative phase analysis was performed using the PowderCell program. For selected samples with relatively high degree of crystallinity the Rietveld refinement was carried out using FullProf.2k (version 5.40) program.

Data on the distribution and chemical nature of elements of lead dioxide deposited at various current densities and deposit thicknesses were obtained by electron Auger spectroscopy at the surface and in several near-surface layers of solid-state atoms. On the energy spectrum of Auger electrons, a qualitative elemental analysis of the surface area irradiated by primary electrons and quantitative analysis of the intensity of the spectral lines were made. The Auger spectra were obtained with a scanning Auger microprobe JAMP-10S, JEOL (Japan) with an accelerating voltage of 10 kV and a beam current of 10^{-8}-10^{-7} A in the element analysis mode. The distribution of elements along the thickness of the coating (homogeneity or heterogeneity of the coating) was determined by layer-by-layer etching. The surface layers were depleted using the built-in ion gun AP-IED2 at an accelerating voltage of 3 kV and an emission of 30 mA. The current density was ~ 200 A cm^{-2}. For ionization, a high-pure Ar was used. For one minute of etching, approximately 20 angstroms of coating are removed. The thickness of the PbO_2 coating for obtaining electron Auger spectra was 20 μm ($S_{Ti\text{-}Pt}$ = 0.5 cm^2) and 2000 μm ($S_{Ti\text{-}Pt}$ = 2 cm^2).

Oxygen evolution reaction was investigated by steady-state polarization on computer controlled EG & G Princeton Applied Research potentiostat model 273A in 0.1M CH_3SO_3H. All potentials were recorded and reported vs. Ag / AgCl / $KCl_{(sat.)}$.

The electrooxidation of organic compounds was carried out in thermostatically controlled divided cell at j_a= 50 mA cm^{-2}. The volume of anolyte was 130 cm^3. Solution, containing phosphate buffer (0.25 M Na_2HPO_4 + 0.1 M KH_2PO_4) + 2×10^{-4} M organic compound, (pH=7.4) was used as electrolyte. Stainless steel was used as cathode. Electrode surface area was 2.5 cm^2. Electrooxidation was conducted on several anodes, such as lead dioxide, lead

dioxide modified by nickel or fluorine ions, obtained both from nitrate and methanesulfonate electrolytes, as well as RuO_2-TiO_2 anode (DSA). The changing of the concentration of dyes and aromatic intermediate products during the electrolysis was measured by sampling (volume of 5 cm^3) at regular intervals and measuring the absorbance of the solution in the ultraviolet and visible region (wavelength range 200-320 nm) using a SF-26 spectrophotometer. Solution, containing phosphate buffer, was used as reference solution. Analyses of the reaction products were conducted by high-performance liquid chromatography (HPLC) using a Shimadzu RF-10A xL instrument equipped with an Ultraviolet SPD-20AV detector and a 30 cm Discovery® C18 column.

3. Results and Discussion

We investigated the degradation of aromatic compounds, namely o- and p-nitroaniline, for determining the electrocatalytic activity of various anode materials. These compounds were chosen as models since they are dangerous pollutants and, additionally, the kinetics of their electrooxidation can be easily studied by UV-vis spectroscopy.

As shown by Borras et al. [15], the overall mechanism for the electrochemical oxidation of aromatic organic compounds involves three consecutive irreversible steps: i) oxidation to a quinoid compound; ii) ring opening reaction with formation of aliphatic acids; iii) mineralization to CO_2 and H_2O. According to literature data [16], a relatively large number of intermediates is formed during the anodic oxidation nitroaniline. Main intermediates are benzoquinone and maleic acid. Only aliphatic acids are detected in the solution after prolonged electrolysis.

The mechanism of p-nitroaniline electrooxidation on modified lead dioxide electrodes was considered in detail in our previous publications [12]. The HPLC investigation has shown 1,4-benzoquinone as the major aromatic intermediate. Only aliphatic acids can be detected in a solution after long-term electrolysis.

We followed the disappearance of intermediate aromatic products as a function of electrolysis time for different concentrations of the initial compound. The mechanism of electrochemical oxidation of the target compound is qualitatively the same for unmodified and modified PbO_2 electrodes; this allows a comparison of electrocatalytic activities in terms process rates which, instead depend appreciably on the electrode material.

Three bands are observed in the spectra of o-nitroaniline (Fig. 1a): i) the E–band (allowed $\pi\rightarrow\pi^*$ transition) at 229 nm: ii) the K–band ($\pi\rightarrow\pi^*$ transition in the conjugated chromophore system) at 275 nm and iii) the B–band ($\pi\rightarrow\pi^*$ transition in the system of a conjugated aromatic chromophore) at 410 nm. Two bands are observed in the spectra of p-nitroaniline (the K band overlaps B, Fig. 2a): the E band at 229 nm, and the K band at 380 nm. The minimum concentration at which all peaks of nitroanilines are clearly visible is 0.2 mM. The concentration of nitroanilines was determined from the absorption maxima on electronic adsorption spectra (ONA – 410 nm, PNA – 380 nm) from the calibration curves (Figs. 1b, 2b).

All chemicals were reagent grade. Lead dioxide anodes were synthesized according to the method described elsewhere. The initial stage of the investigations, a RuO_2-TiO_2 anode (DSA) was chosen as the anode material, which has a low oxygen overvoltage and a relatively low electrocatalytic activity in the oxidation of organic substances. As follows from the obtained data (Fig. 3), nitroaniline is electrochemically oxidized on DSA. The oxidation process is satisfactorily described by zero order reactions, which indicates a significant role of the adsorption stage of the heterogeneous catalytic process. There is every reason to believe that this process is a typical reaction with oxygen transfer, which occurs with the participation of oxygen- containing radicals adsorbed on the electrode. It is noteworthy that the rate constant of oxidation of p-nitroaniline (4.39×10^{-7}) is lower than for o-nitroaniline (4.73×10^{-7} mol dm^{-3} min^{-1}). Correlation coefficients are 0.998 and 0.993, respectively.

It is recognized that the effectiveness of the electrooxidation of organic pollutants depends, first of all, on the anode material, the electrolyte nature, as well as on the structure and composition of the toxicant [17]. The application of anode materials based on lead dioxide represents considerable scientific and practical interest due to the high stability and low cost of anodes and their high electrocatalytic activity in reactions occurring at high anode potentials with the oxygen-containing radicals participation [12−14].

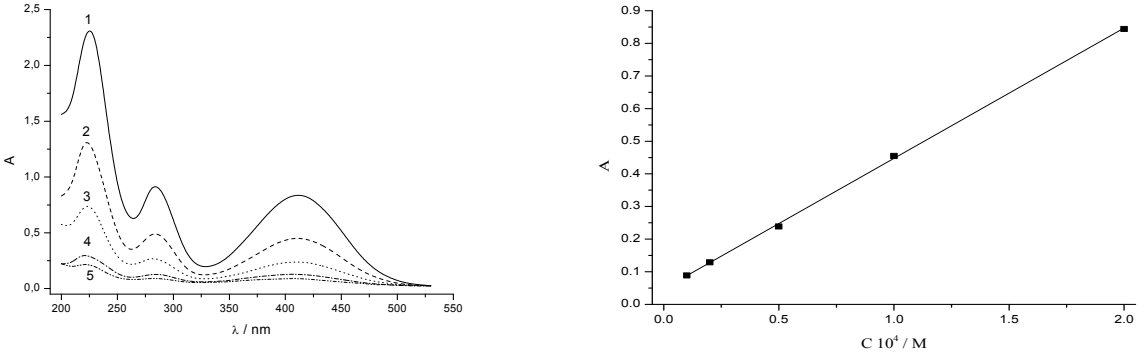

a b

Fig. 1. (a) The absorption spectra of o-nitroaniline solution in a phosphate buffer: 1 – 2×10^{-4}; 2 – 1×10^{-4}; 3– 5×10^{-5}; 4 – 2×10^{-5}; 5 – 1×10^{-5} M; (b) calibration curve for determination of the concentration of o-nitroaniline, λ = 410 nm.

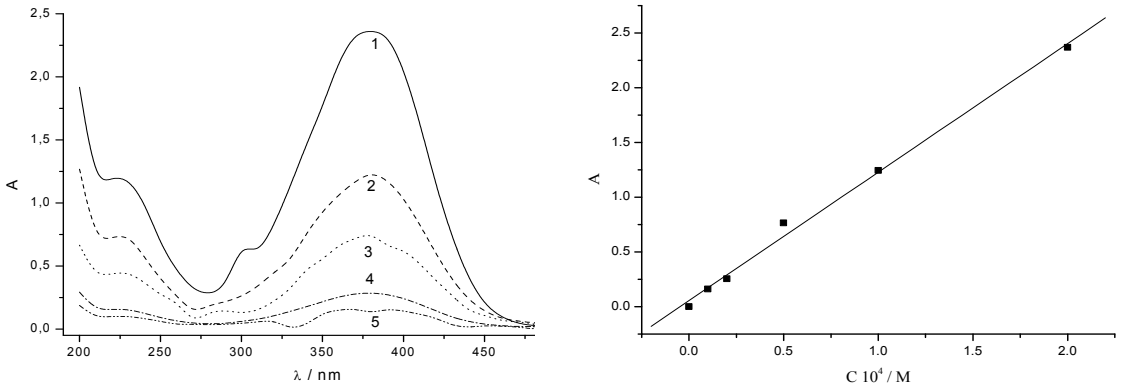

a b

Fig. 2. (a) The absorption spectra of p-nitroaniline solution in a phosphate buffer: 1 – 2×10^{-4}; 2 – 1×10^{-4}; 3– 5×10^{-5}; 4 – 2×10^{-5}; 5 – 1×10^{-5} M; (b) calibration curve for determination of the concentration of p-nitroaniline, λ = 380 nm.

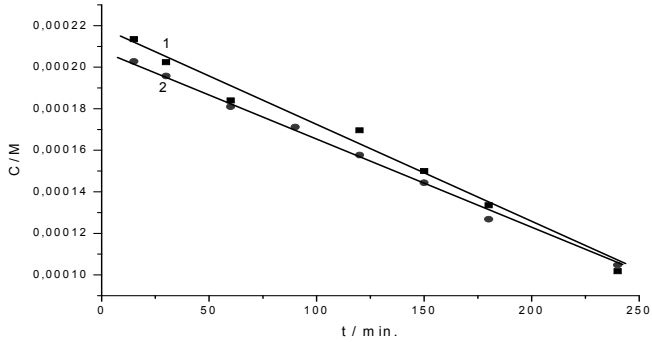

Fig. 3. Kinetic curves of electrooxidation of nitroaniline on DSA: 1 – ONA; 2 – PNA.

In this regard, in order to increase the efficiency of the process, we chose a lead dioxide anode, which has proved to be an effective electrocatalyst for the processes of oxidation of organic substances of various nature. As one can conclude from Fig. 4, oxidation of nitroaniline can also be described by the kinetic equation for zero order reactions. In this case, the rate constants of the reaction increase almost 3-fold, but the difference between the ortho- and para-nitroaniline is still conserved. The rate constant of oxidation of p-nitroaniline (1.42×10^{-6}) is lower than for o-nitroaniline (1.68×10^{-7} mol dm^{-3} min^{-1}). Correlation coefficients are 0.998 and 0.995, respectively.

As it has been displayed in previous publications of our group [12–14], the introduction of small amounts of certain ions into the deposition electrolyte results in a change in regularities of lead dioxide electrodeposition as well as in the physico-chemical properties of obtained coatings. It is believed that the effect of ionic additives on the electrodeposition of lead dioxide is due, on the one hand, to their effect on the ratio of the inert and labile forms of oxygen-containing particles adsorbed on the surface, and, on the other hand, to a change in the nature of the Pb(II) discharged particles.

The presence of fluoride ions in the electrolyte made it possible to significantly expand the range of current densities in which the deposition of lead dioxide proceeds with a 100% current efficiency, which is especially important in the synthesis of coatings with a considerable thickness (several millimeters).

The fluoride ion is easily incorporated into the structure of lead dioxide, replacing the hydroxyl groups in the hydrated zone and thereby affecting the texture and morphology of the resulting coating.

When fluoride ion is added into the electrolyte, the deposition of lead dioxide begins at more positive potentials compared to the base electrolyte. However, when the content of F-ions in the electrolyte is small (0.001-0.010 M), there is no noticeable change in the deposition rate of lead dioxide. When the concentration is increased to 0.01-0.05 M NaF, a slight inhibition of the deposition process of lead dioxide is observed [18].

Fluoride ions are included in the growing oxide, as evidenced by the XPS measurements and Auger spectroscopy. The fluorine content in the coating varies from 2 to 4 at.%, depending on the composition of the electrolyte, the deposition conditions and the thickness of the coating.

As one can see from X-Ray diffractogramm of lead dioxide deposited from electrolytes containing F^- ions differs significantly from PbO_2, the latter was discussed in details in our previous paper [13]. Despite the deposition at room temperature, lead dioxide almost entirely consists of the β-phase represented by the crystallographic orientations (110), (101), (211), (301), (321), where the orientation (101) is preferred.

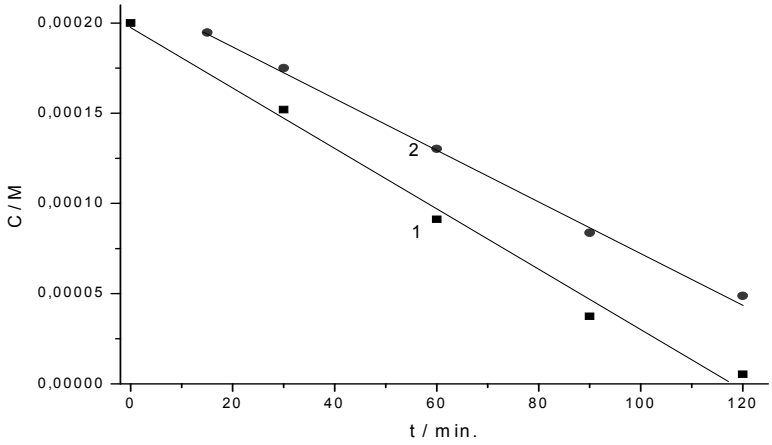

Fig. 4. Kinetic curves of electrooxidation of nitroaniline on PbO_2: 1 – ONA; 2 – PNA.

In the presence of fluoride ions, a significant increase in the intensity of the peaks is observed, indicating an increase in the crystallinity of the obtained coating (Figs. 5a, 5b). As the temperature was raised to 75° C, only the β-phase was found in the lead dioxide deposit, with a change in the crystallographic orientation (the preferred orientation in this case is (101) facet) and a significant increase in the intensity of the peaks (β-phase (110), (211),

(301)) on the diffractogramm. It was found that with an increase in the fluoride ion content to 0.06 M in the deposition electrolyte, a predominant growth of the crystallographic orientation of (211) facet is observed. The obtained data indicate an increase in the crystallinity of lead dioxide in the presence of fluoride ions and high temperature.

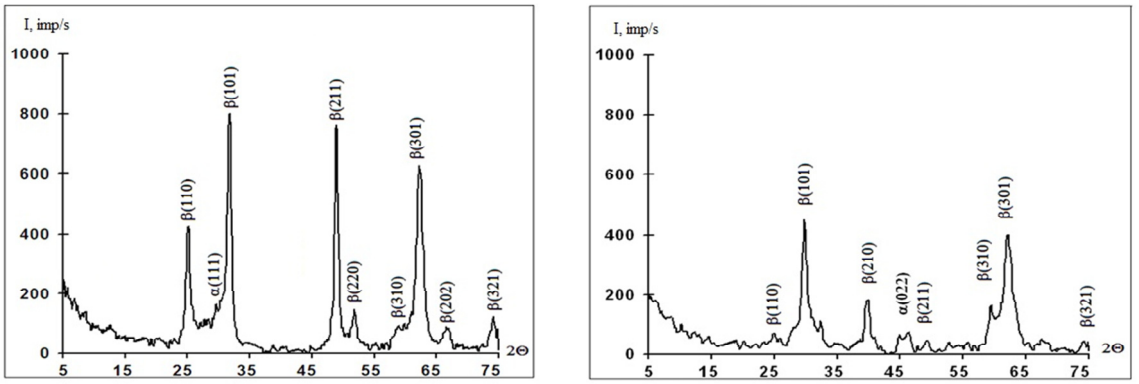

Fig. 5. X-Ray diffractogramm (Cu-K_α) of lead dioxide, deposited on Ti-Pt electrode from (a) 0.1 M $Pb(CH_3SO_3)_2$ + 0.1 M CH_3SO_3H+0.02 M NaF, j_a=10 mA cm^{-2}; (b) 1 M $Pb(CH_3SO_3)_2$ + 0.1 M CH_3SO_3H+0.02 M NaF, j_a=40 mA cm^{-2};t=22° C.

To get further insight on the influence of fluoride ions on the chemical composition of lead dioxide, F-PbO_2 samples of different thicknesses were obtained. Figure 6 displays the F *KLL* Auger spectrum of lead dioxide, which shows that the spectrum consists of three main well-resolved groups of lines (bands) in the regions I – 643 eV, II – 653 eV and III – 667 eV. The mutual ratio of the intensities of these groups of lines I and II in the spectra of F *KLL* in the fluorine-containing compound in comparison with the reference substance NaF corresponds to 10 eV and indicates the inclusion of fluoride ions in the structure of lead dioxide (see Fig. 6, ii). As indicated in [18], the introduction of F- ions in PbO_2 leads to a significant decrease in the amount of crystallization water in the oxide. This is due to the replacement of hydroxyl groups that compensate the charge of Pb^{2+} ions in the hydrated zone of oxide, on F^- by the ion exchange mechanism. Such a process does not require significant energy inputs, since the charges and ionic radii of the hydroxyl groups and the fluoride ions practically do not differ [18].

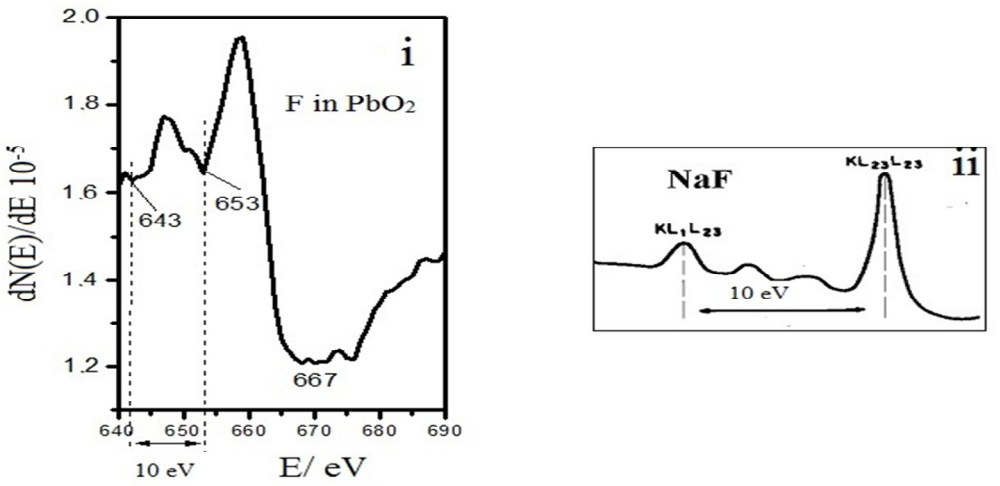

Fig. 6. *KLL* Auger spectra. i) Fluorine in PbO_2, deposited on platinized titanium from 1 M $Pb(CH_3SO_3)_2$ + 0,1 M CH_3SO_3H+0,06 M NaF at j_a=80 mA cm^{-2}; ii) NaF.

As one can see from Fig. 7, atomic concentrations of the elements in the coating do not change during the coating growth. The constant atomic concentration of the F-ion over the entire thickness of the coating indicates the incorporation of the anion, during the growth of the coating, from the initial stages of formation of the active mass.

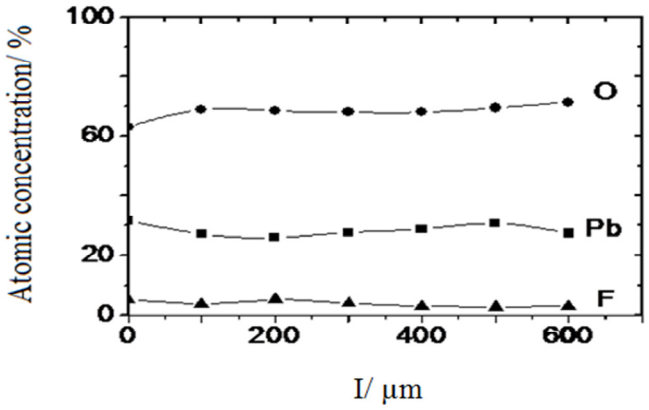

Fig. 7. Atomic concentrations of elements along the depth of the F-PbO_2 sample, after fracture of a deposit with a thickness of 2000 μm in vacuum. The spectra were taken at a point every 100 μm from the edge of the sample.

Modification of the lead oxide by fluoride ions results in an increase in the overvoltage of the oxygen evolution reaction (OER). Moreover, the OER overvoltage is affected not so much by the presence of fluoride ions in the solution, but to a greater extent by the surface state of the lead dioxide formed in the presence of these ions. Fluoride ions are included in the deposit; modify it, changing, probably, the ratio of labile and inert forms of oxygen on its surface. Figure 8 displays that oxygen evolution on F-PbO_2 from 0.1 M CH_3SO_3H solution occurs at more positive potentials. Addition of 0.001 M NaF into this electrolyte practically does not change the OER overvoltage (Fig. 8, curves 2, 3).

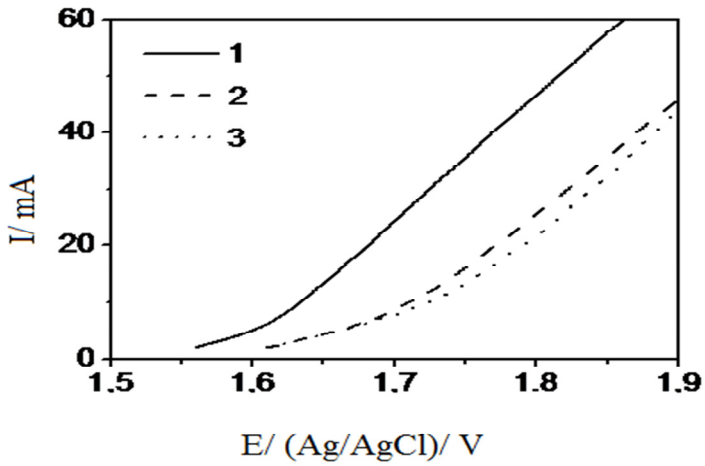

Fig. 8. Steady state polarization curves of oxygen evolution on PbO_2-based electrodes deposited from 0.1 M $Pb(CH_3SO_3)_2$+0.1 M CH_3SO_3H (1); 0.1 M $Pb(CH_3SO_3)_2$+0.1 M CH_3SO_3H+0.001 M NaF (2, 3). Supporting electrolyte 0.1M CH_3SO_3H (1, 2) and 0.1 M CH_3SO_3H+0.001 M NaF (3). v=1 mV s^{-1}.

When using F-PbO_2, the rate of oxidation of nitroaniline increases almost 3-fold as compared to unmodified lead dioxide. At the same time, all the regularities remain the same as those observed for DSA and PbO_2. The oxidation

process is satisfactorily described by zero-order reactions, which indicates the significant role of the adsorption stage of the heterogeneous catalytic process. The rate constant of oxidation of p-nitroaniline (4.59×10^{-6}) is lower than for o-nitroaniline (4.93×10^{-7} mol dm^{-3} min^{-1}.)). Correlation coefficients are 0.997 and 0.999, respectively. It is noteworthy that the use of F-PbO_2-anodes instead of DSA allows more than an order of magnitude to increase the rate of oxidation of nitroaniline.

Conclusions

The processes of electrochemical oxidation of nitroanilines on nonmodified and modified lead dioxide and DSA electrodes occur qualitatively the same and differ only in the rate. This suggests the invariability of the mechanism of their oxidation on different materials that allows one for a correct comparison of their electrocatalytic activity.

According to calculations, based on kinetic studies of the reaction rate constant of degradation depends on the composition of the electrode material and rises significantly in the case of F-doped lead dioxide.

The maximum interest for the electrochemical destruction of nitroanilines represents lead dioxide electrodes modified by fluorine to which a rate constant of p-nitroaniline oxidation increases in 3 times compared with nonmodified electrodes.

References

[1] K. Naseem, R. Begum, Z.H. Farooqi Catalytic reduction of 2-nitroaniline: a review, Environ. Sci. Pollut. Res. Int. 24 (2017) 6446–6460.
[2] P Aravind, H. Selvaraj, S. Ferro, G.M. Neelavannan, M. Sundaram, J. Clea. Prod. 182 (2018) 246–258.
[3] B. P. Chaplin, Environ. Sci.: Processes Impacts 16 (2014), 1182–1203.
[4] E. Brillas, C. A. Martinez-Huitle, Appl Catal., B, 166–167 (2015), 603–643.
[5] M. A. Oturan, J.-J. Aaron, Crit. Rev. Env. Sci. Tech. 44 (2014) 2577–2641.
[6] C.A. Martinez-Huitle, E. Brillas, Appl. Catal., B 87 (2009) 105–145.
[7] M.A. Oturan, M. Pimentel, N. Oturan I. Sires, Electrochim. Acta, 54 (2008) 173–182.
[8] R. Vargas, C. Borras, D. Mendez, J. Mostany, B.R. Scharifker, J. Solid State Electrochem., 20 (2016) 875–893.
[9] A. W. Vermilyea, B. M. Voelker, Environ. Sci. Technol. 43 (2009) 6927-6933.
[10] J.-H. Sun, S.-P. Sun, M.-H. Fan, H.-Q. Guo, Y.-F. Lee, R.-X. Sun, J. Hazard Mat. 153 (2008) 187–193.
[11] D. S. Lee, K. S. Park, Y. W. Nam, Y.-C. Kim, C. H. Lee, J. Hazard Mat. 56 (1997) 247–256.
[12] O. Shmychkova, T. Luk'yanenko, A. Yakubenko, R. Amadelli, A. Velichenko, Appl. Catal., B 162 (2015) 346–351.
[13] O. Shmychkova, T. Luk'yanenko, R. Amadelli, A. Velichenko, J. Electroanal. Chem. 774 (2016) 88–94.
[14] O. Shmychkova, T. Luk'yanenko, R. Amadelli, A. Velichenko, J. Electroanal. Chem. 706 (2013) 86–92.
[15] C. Borras, T. Laredo, J. Mostany, B.R. Sharifker, Electrochim. Acta 49 (2004) 641–648.
[16] N. E. Jimenez Jado, C. Fernandez Sanchez, J. R. Ochoa Gomez, J. Appl. Electrochem. 34 (2004) 551–556.
[17] E. Brillas, B. Boye, M. Banos, J. Calpe, J. Garrido, Chemosphere 51 (2015) 227–235.
[18] R. Amadelli, L. Armelao, E. Tondello, S. Daolio, M. Fabrizio, C. Pagura, A. Velichenko, Appl. Surf. Sci. 142 (1999) 200–203.